

# Microbubble-Based Fiber Optofluidic Interferometer for Sensing

Chen-Lin Zhang, Yuan Gong, Wen-Liang Zou, Yu Wu, Yun-Jiang Rao, *Fellow, IEEE, Fellow, OSA*,  
Gang-Ding Peng, *Fellow, OSA*, and Xudong Fan, *Fellow, OSA*

**Abstract**—A fiber optofluidic interferometer based on an optical microbubble-on-tip ( $\mu$ BoT) structure is developed. The generation process and sensing mechanism of this  $\mu$ BoT sensor are very different from traditional optical fiber sensors. The  $\mu$ BoT is a hybrid solid/liquid/gas microstructure generated by heating a fiber tip with laser and can be easily regenerated with low cost and good repeatability. Carbon nanotube film is optically deposited on the fiber end face to increase the laser absorption, thus enhances the efficiency of the  $\mu$ BoT generation. The diameter of the  $\mu$ BoT interferometer increases with time, leading to a decrease in the free spectral range (FSR). By measuring the FSR, the temperature and flow rate sensing are demonstrated. A temperature sensitivity of  $-1146 \text{ pm}/^\circ\text{C}$  is achieved, which is two orders of magnitude higher than that of the widely used fiber Bragg gratings. A lower limit of detection of  $10 \text{ nL}/\text{min}$  and a resolution of  $0.03 \text{ nL}/\text{min}$  for the flow rate sensing are obtained, which is better than that of the state-of-the-art microfluidic flowmeters. Our study will open a door to the development of novel reconfigurable fiber optofluidic sensors.

**Index Terms**—Fiber optic sensors, interference, optofluidics.

## I. INTRODUCTION

TRADITIONAL optical fiber sensors (OFS) such as fiber Fabry-Perot (FFP) [1] and fiber Bragg grating (FBG) sensors [2] were invented decades ago and have been fabricated in optical fibers by various micromachining technologies [3]–[5]. In addition, various materials [6], [7] were incorporated with optical fibers to enhance the sensing performance or to extend the versatility. However, all these OFS were based on pure solid

materials, which inherently have drawbacks of low flexibility and are lack of reconfigurability.

Combining optofluidics [8]–[11] with optical fiber sensors leads to a new research topic, i.e., the so-called fiber optofluidic (FoF) sensors [12], [13]. Previous efforts were made on the FoF sensors by using conventional OFS to detect analyte in the microfluidic environment. Recently, people started to develop FoF sensors by employing the unique properties of the non-solid materials for reconfigurability [11]. Bykov *et al.* developed a flying particle sensor by optically trapping a single microparticle in air within the hollow-core photonic crystal fiber [12]. Gong *et al.* demonstrated a sensitive FoF flow rate sensor by using a trapped microparticle in water [13]. Based on the non-solid materials and optical forces, these sensors were entirely different in operating principle from traditional OFS.

Recently microbubbles with solid shell were developed by precise fusion splicing method and very high sensitivity for strain sensing was demonstrated [5]. Sumetsky *et al.* also reported a solid microbubble resonator based on a micro capillary [14]. The device cannot be changed once it was produced. In this paper, we proposed and demonstrated a reconfigurable fiber optofluidic sensor based on a gas microbubble in liquid, which was generated by laser heating on a fiber tip ( $\mu$ BoT) in the microfluidic environment. Our studies show that the  $\mu$ BoT generation is simple, highly reproducible, and of low cost. The  $\mu$ BoT acts as a micro-interferometer, which can be used to detect temperature and flow rate with superior performance.

## II. EXPERIMENTAL SETUP AND PRINCIPLE

Experimentally, two laser beams were delivered to the same fiber tip through a wavelength division multiplexer (WDM). A heating beam at  $980 \text{ nm}$  was employed to heat microfluid and generated the microbubble on the fiber tip. The laser power was tunable from  $0$  to  $300 \text{ mW}$ . A tunable laser from an optical spectrum analyzer (OSA) (OPT162,  $1505 \text{ nm}$ – $1630 \text{ nm}$ , Agilent) was used to monitor the changes of the reflective interference spectra that resulted from the evolution of the microbubble. The interference occurred between the Fresnel reflections from the solid/air surface and the other from the air/liquid surface.

Even though a bare single mode fiber (SMF) tip is sufficient to generate a  $\mu$ BoT, a large heating laser power is required. To reduce the power, a carbon nanotube (CNT) film was deposited on the fiber tip to increase the absorption of pump laser, thus easing the  $\mu$ BoT generation [15], [16].

Manuscript received February 24, 2017; revised April 18, 2017; accepted April 19, 2017. Date of publication April 23, 2017; date of current version May 15, 2017. This work was supported in part by the National Natural Science Foundation of China (61575039), in part by the Fundamental Research Funds for the Central Universities (ZYGX2015 J137), and in part by the 111 Project (B14039) (Corresponding author: Yuan Gong.).

C.-L. Zhang, W.-L. Zou, Y. Wu, and Y.-J. Rao are with the Key Laboratory of Optical Fiber Sensing and Communications, Ministry of Education, University of Electronic Science and Technology of China, Chengdu 611731, China (e-mail: 1045020063@qq.com; zouwenliang163@163.com; wuyuzju@163.com; yjrao@uestc.edu.cn).

Y. Gong is with the Key Laboratory of Optical Fiber Sensing and Communications, Ministry of Education, University of Electronic Science and Technology of China, Chengdu 611731, China, and also with the Department of Biomedical Engineering, University of Michigan, Ann Arbor, MI 48109 USA (e-mail: ygong@uestc.edu.cn).

G.-D. Peng is with the School of Electrical Engineering and Telecommunications, University of New South Wales, Sydney, N.S.W. 2052, Australia (e-mail: g.peng@unsw.edu.au).

X. Fan is with the Department of Biomedical Engineering, University of Michigan, Ann Arbor, MI 48109 USA (e-mail: xsfan@umich.edu).

Color versions of one or more of the figures in this paper are available online at <http://ieeexplore.ieee.org>

Digital Object Identifier 10.1109/JLT.2017.2696957

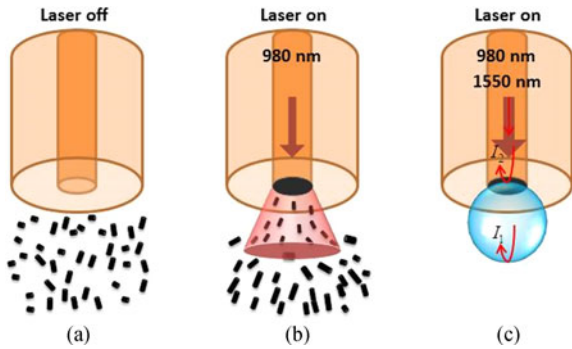


Fig. 1. Formation of the fiber optofluidic microbubble-on-tip sensor. CNTs were randomly distributed in solution with 980 nm laser switched off (a) and can be deposited near the fiber core area with the laser on (b). The  $\mu$ BoT structure, acting as a micro-interferometer, can be generated with a laser pump at 980 nm (c), while using a probe beam at the 1550 nm band for spectral analysis.

We chose CNT because it has a low conductivity of  $\sim 1.52$  W/(m·K) in the radial direction and also a low specific heat capacity of  $0.7$  J/(g·K) [17], [18], which are helpful for increasing the absorption of pump laser and introducing a large temperature increment for the  $\mu$ BoT generation. The coating process is simple, as described below. First an SMF was cleaved, washed with DI water, and dried under an ultraviolet (UV) irradiation ( $90$  mW/cm<sup>2</sup>) for 20 min. Then the fiber tip was inserted into the CNT solution 2 cm below the solution surface. The CNT working solution was obtained by diluting  $18$   $\mu$ L of CNT stock solution (9.0 w.t.% multiwall carbon nanotubes (MWNTs) and 1.8 w.t.% dispersant TNWDIS, Timesnano Inc.) in 10 mL of deionized (DI) water. At the beginning, the CNTs in the solution were randomly distributed, as illustrated in Fig. 1(a). Then a continuous-wave (cw) 980 nm diode laser was switched on with a power of 20 mW and the CNTs were coated on the fiber tip [19] (see Fig. 1(b)) for 15 min. While keeping the laser on, the fiber tip was pulled out of the CNT solution at a slow speed of 0.01 mm/s and the residual solution on the tip was air-dried to solidify the CNT film and to improve the stability of the film for sensing. The efficiency of the deposition was improved during the pulling out process due to the local thermal effect near the surface of the solution [20].

The coated fiber tip was inserted into a microfluidic channel with a cross-section of  $300$   $\mu$ m  $\times$   $300$   $\mu$ m, in which the deionized (DI) water was flowed through. When the laser power was absorbed by the CNTs, a sharp temperature rise was generated in a very low volume near the fiber tip. A microbubble was generated thanks to the increment of the gas content around the fiber tip, either from the separation of dissolved gas from the liquid or from the vaporization of the liquid as the temperature increased (see Fig. 1(c)). Then the microbubble kept on growing if the pump laser power was sustained. The growth rate of the microbubble would change when the ambient parameters change. The FSR of the microbubble at a fixed heating time was used as the sensing signal. For temperature sensing, the gas for microbubble mainly came from the vaporization of the liquid, similar to boiling the water by heating. For flow rate sensing, the gas mainly came from dissolved gas delivered together with the microfluid and can be refreshed as the fluid flows. High

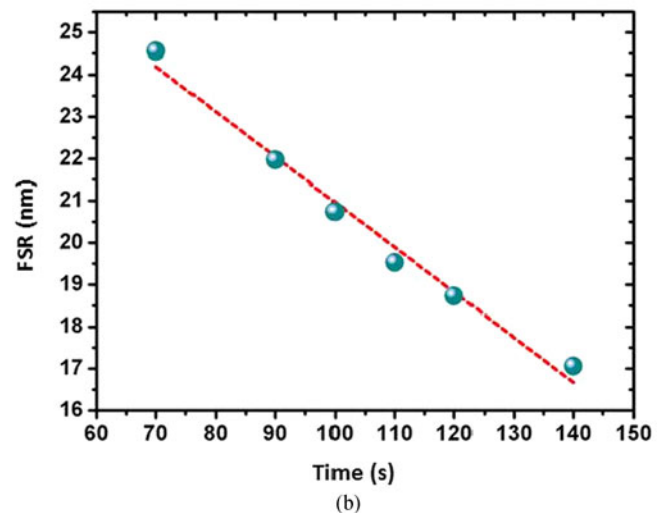
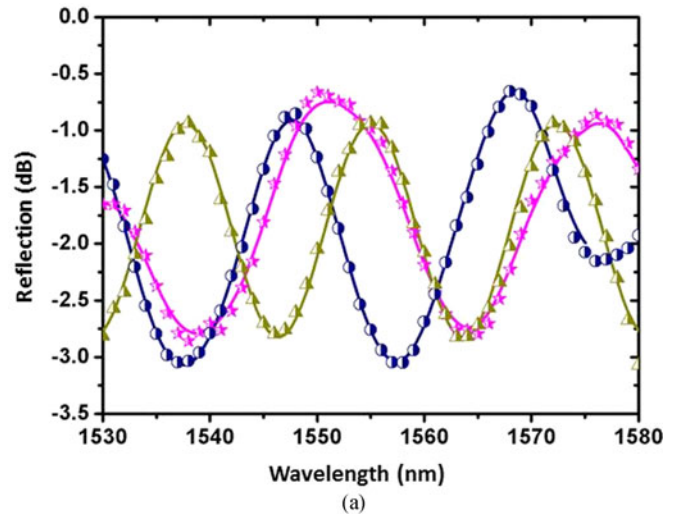


Fig. 2. (a) The interference spectra of the fiber optofluidic microbubble-on-tip structure and (b) FSR versus heating time.

sensitivity was achieved thanks to the photothermal effect of CNT and the small volume of the microbubble.

The reflective spectra from the  $\mu$ BoT structure at heating time of 70 s, 100 s and 140 s are shown in Fig. 2(a), while the ambient temperature was kept constant. The laser power for heating was 221 mW. The fringe contrast was not as high as solid fiber micro-interferometers, but was sufficient to determine the free spectral range (FSR) of the interference spectra. A compromise between increasing the absorption by CNTs and keeping good interference fringes should be considered during the CNTs deposition. The FSR decreases with a good linearity ( $R^2 \sim 0.98$ ) as the microbubble grows in time (see Fig. 2(b)).

The diameter of the microbubble was also monitored by a charge-coupled device (CCD) camera. An example of the temporal evolution of the microbubble is shown in Fig. 3. Three microscopic images of the microbubbles, corresponds to that of the spectra in Fig. 2(a), are shown in the inset of Fig. 3. There was a sharp nonlinear increase in diameter at the beginning because a fast temperature rise was obtained when the laser was switched on. Then the diameter increased with time with a good

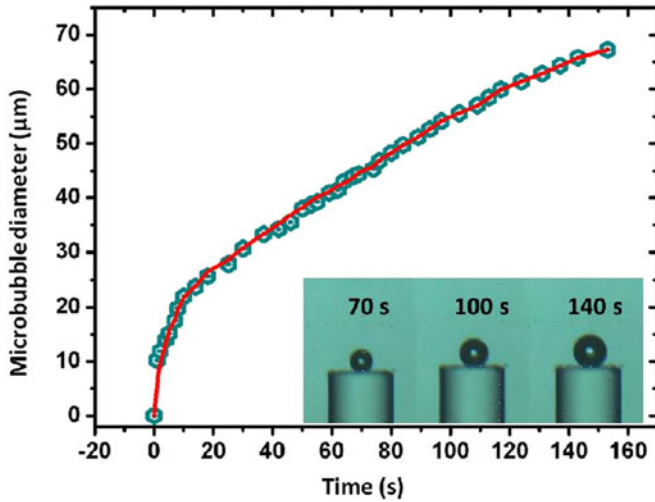


Fig. 3. The generation of the fiber optofluidic microbubble-on-tip for 150 s.

linearity ( $R^2 \sim 0.99$ ) between 50 s and 150 s. When the diameter was large, the temperature rise became slow and gradually got balanced. Since the FSR changed linearly over certain range of heating time, detecting FSR in this time range would not influence on the calibration curve for sensing.

The FSR can be expressed by  $FSR = \lambda_1 \lambda_2 / (2nL_{eff})$ , with  $n$  and  $L_{eff}$  the refractive index and the effective length of the microbubble interferometer, respectively. The FSR is inversely proportional to the diameter of the microbubble. Therefore, in principle, measuring the FSR is equivalent to detecting the diameter of the microbubble by a CCD camera. For the  $\mu$ BoT-based sensing, the imaging detection method is more cost-effective, while the spectroscopic detection method has higher resolution. Here, we would employ the spectral detection method to achieve higher sensing performance. As the microbubble in our experiment grows with a relative slow speed, the measurement time of FSR, which can be determined easily within sub-100 ms level, can be neglected and will not influence the sensing performance.

### III. RESULTS AND DISCUSSION

Ambient temperature measurement was demonstrated by the  $\mu$ BoT sensor. The fiber was fixed with the microfluidic chip and the whole chip was immersed into a thermostatic water bath for temperature calibration. The microfluid did not flow in the temperature sensing experiment. At each temperature, the 980 nm laser was turned on with a power of 146 mW and the reflective spectra of microbubble was recorded after heating for 60 s. Fig. 4(a) shows the FSR changes as a function of the temperature. Temperature was measured between 25 °C and 45 °C, which covers the temperature range of human body and is significant for the human-on-a-chip or organ-on-a-chip applications [21], [22]. Note that the temperature measured here is not only that of the microfluid, but the ambient temperature. In most microfluidic applications, the reagents are firstly warmed up to the room temperature so that the temperature of the microfluid is usually the same as the ambient temperature.

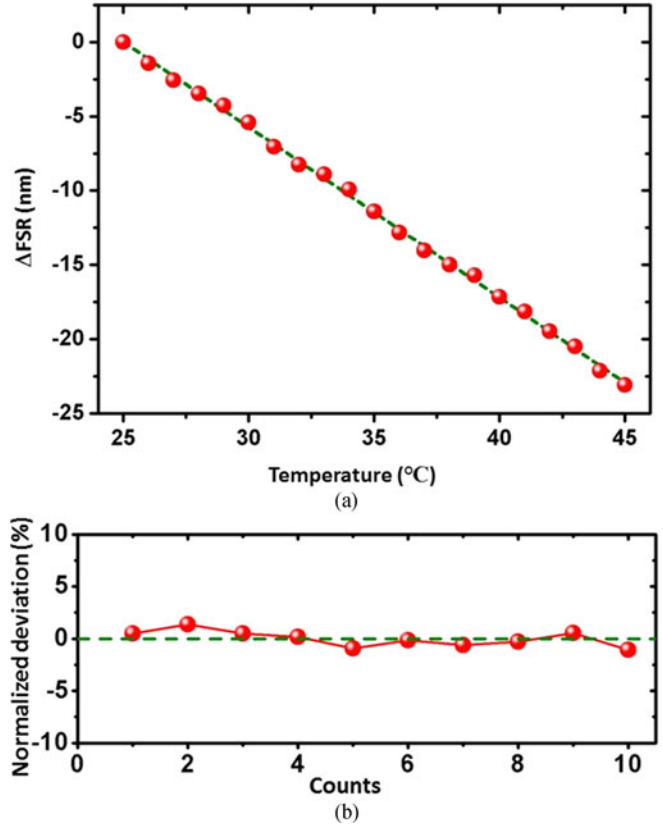


Fig. 4. (a) FSR changes versus temperature with a heating time of 60 s at 146 mW of 980 nm pump and (b) the repeatability of the same probe for 10 tests.

At higher temperature, the microbubble is larger so that the FSR is smaller.

A good linearity ( $R^2 \sim 0.998$ ) is achieved and the sensitivity is  $-1146 \text{ pm}/^\circ\text{C}$ , two orders of magnitude higher than FBGs [23]. The sensitivity ( $\delta$ ) is determined by the slope of the linear fitting curve from data in Figs. 4(a),  $\delta = \Delta y / \Delta x$ .  $x$  is the parameter to be tested and  $y$  is the output signal,  $\Delta FSR$  in this work. By using the same probe, good repeatability was confirmed by 10 times of tests at 25 °C. Between two tests, the pump laser was switched off to let the microbubble disappear. The FSR was statistically determined to be  $29.358 \pm 0.224 \text{ nm}$ , corresponding to a deviation of  $\pm 0.76\%$  (see Fig. 4(b)). The deviation of FSR was calculated by  $D = (FSR - \overline{FSR}) / \overline{FSR} \times 100\%$ , where  $\overline{FSR}$  was the statistically averaged FSR over 10 tests. The accuracy can be roughly evaluated by the statistical deviation of  $\pm 0.76\%$ . The theoretical temperature resolution can be determined to be about  $0.002 \text{ }^\circ\text{C}$  by the sensitivity of  $1146 \text{ pm}/^\circ\text{C}$  and the spectral resolution of 2 pm. Then three different probes were tested for temperature sensing, indicating good consistency in the sensor's fabrication process (see Fig. 5). The fluctuation might be from the instability of CNT film after many times of tests, as well as the instability of the syringe pump and the microfluid, limiting the accuracy of the sensor. It can be improved by optimizing the deposition process, such as drying for a relatively long time after coating or improving the

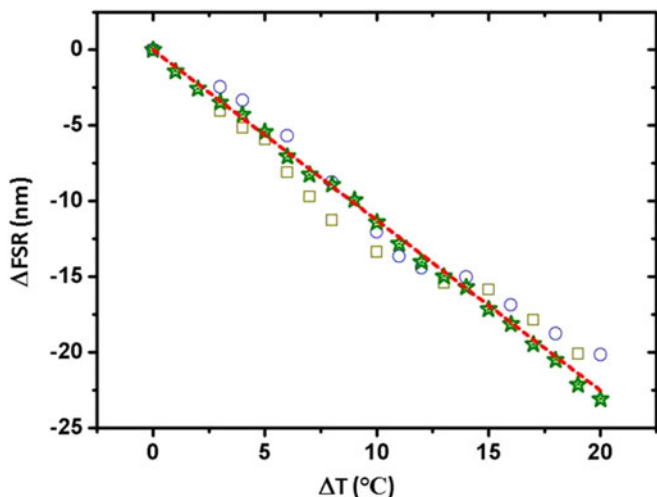


Fig. 5. Repeatability of the calibration curves for three different  $\mu$ BoT temperature probes.

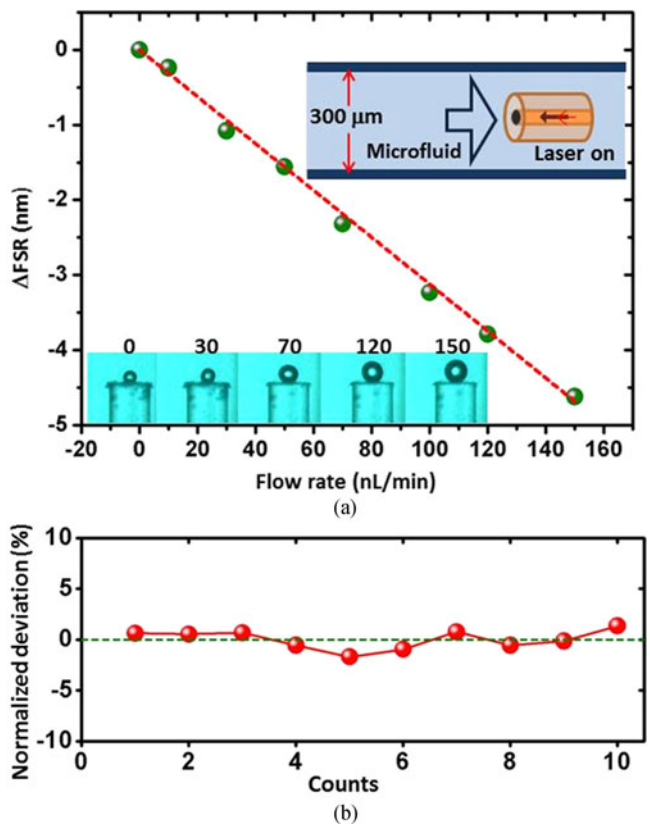


Fig. 6. (a) FSR changes as a function of flow rate with a heating time of 120 s at 221 mW of 980 nm pump and (b) the repeatability of the same probe for 10 tests.

adherence strength by an interlayer between fiber face and the CNT film.

For the microfluidic flow rate sensing, we used a syringe pump (Harvard Apparatus) to precisely control the microfluid, which flowed toward the fiber tip, as shown in the insert of Fig. 6(a). The stability of the syringe pump is very good so that the flow rate variation can be neglected. The fiber was adjusted to the center of the cross section in the microchannel. We used

a pump power of 221 mW. The FSR, recorded at a heating time of 120 s, is shown as a function of the flow rate in Fig. 6(a). Flow rate of 0 – 150 nL/min was measured. The inset shows the microscopic images of  $\mu$ BoTs under 0, 30 nL/min, 70 nL/min, 120 nL/min and 150 nL/min, respectively. This flow rate range is important for the microfluidic applications such as separation-based sensing of neurotransmitters and certain quick analysis system [24], [25]. A good linearity ( $R^2 \sim 0.997$ ) is achieved and the sensitivity is  $-31 \text{ pm}/(\text{nL}/\text{min})$ , which is determined by the slope of the linear fitting curve. The spectral resolution of the OSA is 1 pm, so the theoretical resolution for the flow rate sensing can be calculated to be as low as 0.03 nL/min, which is much better than the state-of-the-art microfluidic flowmeters with resolution at nanoliter-per-minute level [13], [26]–[28]. 10 times of tests were performed with a flow rate of 120 nL/min and good repeatability was achieved, with a statistical deviation of  $\pm 0.94\%$  (see Fig. 6(b)). The deviation is low and acceptable for sensing. The deviation may originate from the instability of the syringe pump or the non-uniformity of the dissolved gas in the microfluid.

In the flow rate sensing experiment, the microfluidic flow takes away part of the laser-generated heat, therefore, the microbubble was supposed to grow slower at higher flow rate. However, the opposite was surprisingly observed, that is, the microbubble grows faster at higher flow rate, leading to a smaller FSR at a fixed heating time (see Fig. 6(a)). The potential explanation is that the dissolved air in the liquid was delivered more efficiently at higher flow rate, leading to a faster growth of the microbubble. Therefore, the air solubility was initialized by ultrasonic bathing in both temperature and flow rate sensing. For practical use, the calibration needs to be performed at first by using the same sample to be test to make sure the air solubility is the same. The upper detection limit of flow rate was constrained by the maximum diameter of the microbubble, which was determined by the balance between the laser-induced heat, the surface tension and the fresh air supply from the microfluid flow.

Generally, the performance of the fiber optofluidic  $\mu$ BoT sensors can be further improved. First, enhancing the fringe contrast of the interference fringes is helpful to precisely determine the wavelength of interference fringes. The fringe contrast can be enhanced by polishing the fiber tip and thus getting a more uniform coating, and/or by using a solution with a large refractive index instead of DI water to increase the Fresnel reflection from the gas/liquid surface. Second, other materials instead of CNTs are worth being explored in order to further enhance the stability, repeatability, and also the lifetime of the sensor. Third, other sensing output, such as the diameter of the microbubble monitored by imaging, can be employed instead of measuring the FSR. Alternatively, the dynamic fringes from the  $\mu$ BoT sensor can also be measured by using a fixed wavelength laser and a photodetector [29], as the effective length of the  $\mu$ BoT changes much faster and larger than that of the traditional solid fiber micro-interferometers. At current stage, the  $\mu$ BoT interferometer was not ready for the simultaneous measurement of temperature and flow rate. Keeping the ambient temperature constant is a good way, since the FSR changes with both temperature and flow rate. Potential methods for dual-parameter

sensing include the sensitivity coefficient matrix method [30], [31], hybrid sensing structure with two mechanisms [32], etc.

#### IV. SUMMARY

A novel type of fiber optofluidic microbubble-on-tip sensor has been developed and is much more sensitive than the traditional solid fiber-optic micro interferometers. By laser heating, the microbubble was generated in liquid with good reconfigurability and repeatability. CNT film was deposited on the fiber tip to enhance the laser absorption and thus improve the efficiency of the microbubble generation. Ultrahigh sensitivities of  $-1146 \text{ nm}/^\circ\text{C}$  and  $-31 \text{ pm}/(\text{nL}/\text{min})$  have been achieved for temperature and flow rate sensing, respectively. In addition to the sensing applications, the liquid-gas interface of the microbubble in liquid might have the potential to act as a chemical microreactor [33].

#### REFERENCES

- [1] K. A. Murphy, M. F. Gunther, A. M. Vengsarkar, and R. O. Claus, "Quadrature phase-shifted, extrinsic Fabry-Perot optical fiber sensors," *Opt. Lett.*, vol. 16, pp. 273–275, 1991.
- [2] K. O. Hill and G. Meltz, "Fiber Bragg grating technology fundamentals and overview," *J. Lightw. Technol.*, vol. 15, no. 8, pp. 1263–1276, Aug. 1997.
- [3] Z. L. Ran, Y. J. Rao, W. J. Liu, X. Liao, and K. S. Chiang, "Lasermachined Fabry-Perot optical fiber tip sensor for high-resolution temperature-independent measurement of refractive index," *Opt. Exp.*, vol. 16, pp. 2252–2263, 2008.
- [4] T. Wei, Y. Han, H. L. Tsai, and H. Xiao, "Miniaturized fiber inline Fabry-Perot interferometer fabricated with a femtosecond laser," *Opt. Lett.*, vol. 33, pp. 536–538, 2008.
- [5] S. Liu *et al.*, "High-sensitivity strain sensor based on in-fiber rectangular air bubble," *Sci. Rep.*, vol. 5, 2015, Art. no. 7624.
- [6] J. Ma, W. Jin, H. L. Ho, and J. Y. Dai, "High-sensitivity fiber-tip pressure sensor with graphene diaphragm," *Opt. Lett.*, vol. 37, pp. 2493–2495, 2012.
- [7] R. C. Jorgenson and S. S. Yee, "A fiber-optic chemical sensor based on surface plasmon resonance," *Sens. Actuators, B*, vol. 12, pp. 213–220, 1993.
- [8] D. Psaltis, S. R. Quake, and C. Yang, "Developing optofluidic technology through the fusion of microfluidics and optics," *Nature*, vol. 442, pp. 381–386, 2006.
- [9] C. Monat, P. Domachuk, and B. J. Eggleton, "Integrated optofluidics: A new river of light," *Nature Photon.*, vol. 1, pp. 106–114, 2007.
- [10] X. Fan and I. M. White, "Optofluidic microsystems for chemical and biological analysis," *Nature Photon.*, vol. 5, pp. 591–597, 2011.
- [11] H. Schmidt and A. R. Hawkins, "The photonic integration of non-solid media using optofluidics," *Nature Photon.*, vol. 5, pp. 598–604, 2011.
- [12] D. S. Bykov, O. A. Schmidt, T. G. Euser, and P. S. J. Russell, "Flying particle sensors in hollow-core photonic crystal fibre," *Nature Photon.*, vol. 9, pp. 461–465, 2015.
- [13] Y. Gong, Q. F. Liu, C. L. Zhang, and Y. Wu, "Microfluidic flow rate detection with a large dynamic range by optical manipulation," *IEEE Photon. Technol. Lett.*, vol. 27, no. 23, pp. 2508–2511, Dec. 2015.
- [14] M. Sumetsky, Y. Dulashko, and R. S. Windeler, "Optical microbubble resonator," *Opt. Lett.*, vol. 35, pp. 898–900, 2010.
- [15] R. Pimentel Domínguez, J. Hernández Cordero, and R. Zenit, "Microbubble generation using fiber optic tips coated with nanoparticles," *Opt. Exp.*, vol. 20, pp. 8732–8740, 2012.
- [16] K. Kashiwagi, S. Yamashita, and S. Y. Set, "Optically formed carbon nanotube sphere," *Opt. Exp.*, vol. 16, pp. 2528–2532, 2008.
- [17] S. P. Heppelstone, A. M. Ciavarella, C. Janke, and G. P. Srivastava, "Size and temperature dependence of the specific heat capacity of carbon nanotubes," *Surf. Sci.*, vol. 600, pp. 3633–3636, 2006.
- [18] S. Sinha, S. Barjani, G. Iannacchione, A. Schwab, and G. Muench, "Off-axis thermal properties of carbon nanotube films," *J. Nanopart. Res.*, vol. 7, pp. 651–657, 2005.
- [19] K. Kashiwagi, S. Yamashita, and S. Y. Set, "In-situ monitoring of optical deposition of carbon nanotubes onto fiber end," *Opt. Exp.*, vol. 17, pp. 5711–5715, 2009.
- [20] Y. Liu *et al.*, "Highly sensitive fibre surface-enhanced Raman scattering probes fabricated using laser-induced self-assembly in a meniscus," *Nanoscale*, vol. 8, pp. 10607–10614, 2016.
- [21] L. Qi, Y. Wu, Y. Ren, T. Ye, L. Lei, and H. Jiang, "AC electrothermal circulatory pumping chip for cell culture," *ACS Appl. Mater. Interfaces*, vol. 7, pp. 26792–26801, 2015.
- [22] N. Beißner, T. Lorenz, and S. Reichl, "Organ on chip," in *Microsystems for Pharmatechnology*. New York, NY, USA: Springer, 2016, pp. 299–339.
- [23] Y. J. Rao, "In-fibre Bragg grating sensors," *Meas. Sci. Technol.*, vol. 8, p. 355, 1997.
- [24] N. A. Cellar and R. T. Kennedy, "A capillary—PDMS hybrid chip for separations-based sensing of neurotransmitters in vivo," *Lab Chip*, vol. 6, pp. 1205–1212, 2006.
- [25] M. Kumemura and T. Korenaga, "Quantitative extraction using flowing nano-liter droplet in microfluidic system," *Anal. Chim. Acta*, vol. 558, pp. 75–79, 2006.
- [26] C. Hoera *et al.*, "A chip-integrated highly variable thermal flow rate sensor," *Sens. Actuators, B*, vol. 225, pp. 42–49, 2015.
- [27] J. Sadeghi, A. H. Ghasemi, and H. Latifi, "A label-free infrared opto-fluidic method for real-time determination of flow rate and concentration with temperature cross-sensitivity compensation," *Lab Chip*, vol. 16, pp. 3957–3968, 2016.
- [28] M. S. Cheri, H. Latifi, J. Sadeghi, M. S. Moghaddam, H. Shahraki, and H. Hajghassem, "Real-time measurement of flow rate in microfluidic devices using a cantilever-based optofluidic sensor," *Analyst*, vol. 139, pp. 431–438, 2013.
- [29] E. Preter, R. A. Katims, V. Artel, C. N. Sukenik, D. Donlagic, and A. Zadok, "Monitoring and analysis of pendant droplets evaporation using bare and monolayer-coated optical fiber facets," *Opt. Mater. Exp.*, vol. 4, pp. 903–915, 2014.
- [30] L. Jin *et al.*, "An embedded FBG sensor for simultaneous measurement of stress and temperature," *IEEE Photon. Technol. Lett.*, vol. 18, no. 1, pp. 154–156, Jan. 2006.
- [31] Y. Gong, T. Zhao, Y. J. Rao, and Y. Wu, "All-fiber curvature sensor based on multimode interference," *IEEE Photon. Technol. Lett.*, vol. 23, no. 11, pp. 679–681, Jun. 2011.
- [32] Y. J. Rao, Z. L. Ran, X. Liao, and H. Y. Deng, "Hybrid LPFG/MEFPI sensor for simultaneous measurement of high-temperature and strain," *Opt. Exp.*, vol. 15, pp. 14936–14941, 2007.
- [33] L. Zhang, J. L. Liu, C. Liu, J. Zhang, and J. L. Yang, "Performance of a fixed-bed biofilm reactor with microbubble aeration in aerobic wastewater treatment," *Water Sci. Technol.*, vol. 74, pp. 138–146, 2016.

**Chen-Lin Zhang** received the B.Sc. degree in optics from the University of Electronic Science and Technology of China, Chengdu, China, in 2013, where she is currently working toward the Ph.D. degree in optics. Her research interests include optical fiber sensors, optical manipulation, and optofluidics.

**Yuan Gong** received the Ph.D. degree in optics from the Institute of Optics and Electronics, Chinese Academy of Sciences, Beijing, China, in 2008. In July 2008, he was employed as a Lecturer with the University of Electronic Science and Technology of China, Chengdu, China, where he has been an Associate Professor since 2011. He was a Visiting Scholar with the University of Michigan, Ann Arbor, USA, from January 2015 to January 2016. He coauthored more than 80 peer-reviewed journal and conference papers and held one U.S. patents and more than 20 Chinese patents. His research interests include optical fiber sensors, optofluidics, and biochemical detection.

**Wen-Liang Zou** is currently working toward the master's degree at the University of Electronic Science and Technology of China, Chengdu, China. His research interests include optical fiber sensors and optofluidics.

**Yu Wu** received the B.Sc. degree from the University of Electronic Science and Technology of China, Chengdu, Sichuan, China, in 2003, and the Ph.D. degree in measurement technology and instruments from Zhejiang University, Zhejiang, China, in 2008. He is currently an Associate Professor with the Key Lab of Optical Fiber Sensing and Communications, Education Ministry of China, University of Electronic Science and Technology of China. His research interests include photonics devices and microfiber sensors.

**Yun-Jiang Rao** (F<sup>r</sup>) received the Ph.D. degree in optoelectronic engineering from Chongqing University, Chongqing, China, in 1990. He joined the Electric and Electronic Engineering Department, Strathclyde University, U.K., as a Postdoctoral Research Fellow during 1991–1992 and the Applied Optics Group in the Physics Department, Kent University, U.K., as a Research Fellow and then a Senior Research Fellow during 1992–1999. From 1999 to 2004, he was a Chang-Jiang Chair Professor with Chongqing University. From 2004, he held the Chang-Jiang Chair Professor with the University of Electronic Science and Technology of China. He is currently the Director of the Key Lab of Optical Fiber Sensing and Communications, Ministry of Education, University of Electronic Science and Technology of China, Chengdu, China. His research interests include fiber-optic sensors and lasers. He is a Fellow of the OSA and the SPIE.

**Gang-Ding Peng** received the B.Sc. degree in physics from Fudan University, Shanghai, China, in 1982, and the M.Sc. degree in applied physics and the Ph.D. degree in electronic engineering from Shanghai Jiao Tong University, Shanghai, China, in 1984 and 1987, respectively. From 1987 to 1988, he was a Lecturer with Jiao Tong University. He was a Postdoctoral Research Fellow with the Optical Sciences Centre of the Australian National University, Canberra, Australia, from 1988 to 1991. He has been with the University of New South Wales, Sydney, N.S.W., Australia, since 1991, was a Queen Elizabeth II Fellow from 1992 to 1996, and is currently a Professor in the same university. His research interests include optical fiber and waveguide devices and optical fiber sensors. He is a Fellow of the OSA and the SPIE.

**Xudong Fan** received the B.S. and M.S. degrees from Peking University, Beijing, China, in 1991 and 1994, respectively, and the Ph.D. degree in physics and optics from Oregon Center for Optics, University of Oregon, Eugene, OR, USA, in 2000. Between 2000 and 2004, he was a Project Leader with 3M Company on fiber optics and photonic sensing devices for biomedical applications. In August 2004, he joined the Department of Biological Engineering, University of Missouri, as an Assistant Professor and was early promoted to an Associate Professor in 2009. In January 2010, he joined the Biomedical Engineering Department, University of Michigan, Ann Arbor, MI, USA. In 2014, he was early promoted to Professor. His research includes photonic bio/chemical sensors, micro-/nanofluidics, and nanophotonics for disease diagnostics and bio/chemical molecule analysis. He was an Associate Editor for the *Optics Express*, and serves as a Member of the Editorial Board for *Lab on a Chip*. He is a Fellow of the OSA, the SPIE, and the Royal Society of Chemistry.